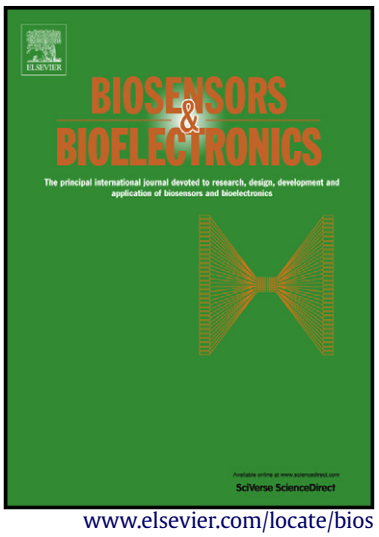

www.elsevier.com/locate/bios

Silicon nanograss based impedance biosensor for label free detection of rare metastatic cells among primary cancerous colon cells, suitable for more accurate cancer staging

Mohammad Abdolahad, Hani Shashaani, Mohsen Janmaleki, Shams Mohajerzadeh

PII: S0956-5663(14)00169-9
DOI: http://dx.doi.org/10.1016/j.bios.2014.02.079
Reference: BIOS6626

To appear in: *Biosensors and Bioelectronics*

Received date: 21 November 2013
Revised date: 27 February 2014
Accepted date: 28 February 2014

Cite this article as: Mohammad Abdolahad, Hani Shashaani, Mohsen Janmaleki, Shams Mohajerzadeh, Silicon nanograss based impedance biosensor for label free detection of rare metastatic cells among primary cancerous colon cells, suitable for more accurate cancer staging, *Biosensors and Bioelectronics*, http://dx.doi.org/10.1016/j.bios.2014.02.079

Silicon nanograss based impedance biosensor for label free detection of rare metastatic cells among primary cancerous colon cells, suitable for more accurate cancer staging

Mohammad Abdolahad [a,*,#], Hani Shashaani[a,#], Mohsen Janmaleki [b,#], Shams Mohajerzadeh [a,*]

[a] Nano Electronic Center of Excellence, Thin Film and Nanoelectronic Lab, School of Electrical and Computer Eng, University of Tehran, Tehran, Iran, P.O. Box 14395/515, Tehran, Iran

[b]Medical Nanotechnology and Tissue Engineering Research Center, Shahid Beheshti University of Medical Sciences P.O. Box 1985717443 Tehran, Iran

***Email : m.abdolahad@ut.ac.ir, mohajer@ut.ac.ir**

[#] Authors with same collaboration

Abstract

Detection of rare metastatic cells within a benign tumor is a key challenge to diagnose the cancerous stage of the patients tested by clinical human biopsy or pap smear samples. We have fabricated and tested a nanograssed silicon based bioelectronic device with the ability of detecting a few human colon invasive cancer cells (SW48) in a mixed cell culture of a primary cancerous colon cells (HT29) without any biochemical labels. A discernible impedance change was elicited after the presence of 5% metastatic cells in whole benign sample. The electric field

penetration as well as current flow to metastatic cells is different from benign ones due to their different membrane dielectric parameters. Beta dispersion as one of intrinsic bioelectrical properties of the cell membrane in blocking the stimulating current flow in the range of kHz is the specific parameter involve in our diagnosis approach. It can reflect depth information about the dielectric properties and the pathological condition of a cell before and after metastatic transformation. Electrically active doped silicon nanograss structures owing their superior nanocontacts with cells membrane can detect any slight variations in current being originated from the presence of rare metastatic cells on the surface of the sensing electrode. The experimental results revealed that bare doped silicon microelectrodes are incapable of resolving different grades of attached cells.

Keywords: silicon nanograss, biosensor, cancer detection, beta dispersion, impedance

1. Introduction

Diagnosis of rare invasive cancer cells among a large amount of benign ones extracted from a suspected tumor is a key challenge to detect the cancerous stage of the disease presented by clinical human biopsy and pap smear samples (Murray et al., 2009). Many biochemical assays have been applied for this trends such as flowcytometry (Ling et al., 2008), magnetic cell separation (Sivagnanam et al., 2010) (Saliba et al., 2010), gene expression such as SNRPF, HNRPAB, DHPS and securin (Alexe et al., 2006), H&E stain (Fischer et al., 2008), electrorotation (Cristofanilli et al., 2002) *etc*. The mentioned methods have many disadvantages such as bio marker labeling complexity and uncertainty, poor efficiencies, high cost and time consuming. Some new investigations in determining the overall biophysical properties and pathophysiological states of a cell specially in cancerous transformation were focused on the electrical analysis of the cell (Mohammad Abdolahad et al., 2012) (Abdolahad et al., 2013b) (Chen et al., 2011). These methods do not require complexities such as sample preparation, biomarker tagging, cell staining, expensive equipment and reagents. In this regard, local invasion and metastatic growth may strongly depend on cell disturbed electrodynamics activity (Pokorný, 2012).

Among various bioelectrical analysis techniques, impedance spectroscopy is a viable alternative method in some point-of-care applications as a noninvasive experiment. Cells that are diseased, cancerous or infected have altered impedance properties (Du et al., 2013)(Hu et al., 2013). These alterations are due to changing cell membrane permeability (Abdolahad et al., 2013b), fluidity (Scaglia et al., 2005), and deformability (Mohammad Abdolahad et al., 2012) along with cell adhesiveness and ion channel activity (Kunzelmann, 2005). The use of dielectric spectroscopy (impedance spectroscopy) to carry out real time observations of cells as well as extract a wealth

of information about their physiological properties has expanded in recent years (Heileman et al., 2013) (Pick et al., 2013) (Vu et al., 2012) (Valero et al., 2010). Dielectric spectra are obtained by applying an electrical signal to cells, which is swept over a frequency range (Lan and Jang, 2011). In the field of cancer diagnosis, cell dielectric data can handle the heterogeneous nature of individual type of the malignancy and distinguish between cells with different metastatic activity due to mentioned alterations. Discriminating cells based on differences in impedance measurements over a wide range of frequencies provide information on cell size, membrane capacitance, cytoplasm conductivity and permittivity as a function of frequency(Asami, 2002)(Cheung et al., 2005). Many investigations distinguish between individual poorly and highly metastatic cancer cells in separated assays by impedance sensors (Heileman et al., 2013)(Han et al., 2007). For example, diagnosis of the oral squamous cell carcinoma (OSCC) cell line and the non-cancerous derived epithelial oesophageal cell line (Het-1A) were measured by a commercially available RT-CES system (Yang et al. 2011). A significant difference between the phase angle of the corresponding impedances of highly and poorly metastatic cells were reported (Frazier et al., 2009). Also recently, biochemical markers (such as histone deacetylase) were applied to diagnose primary and invasive breast cancer cells based on bioimpedance measurements (Srinivasaraghavan et al., 2012). Selectivity and high cost of these markers are challenges which have limited their applications.

Although the bioimpedance character of normal and malignant cells is known to differ, the ability to electrically detect the presence of rare metastatic cells label freely in an unknown staged tumor cells extracted by biopsy or pap-smear as a critical stage in clinical assays has not been yet achieved. This seems to originate from the weakness of microelectrodes of impedance

biosensors in label-free distinguishing the response of the device in the presence or absence of rare metastatic cells (when have been hidden between non metastatic ones). Previously reported impedance electrodes could not detect the electric field distribution altered by such a low metastatic cells in a flow of field lines passed from large amount of benign cells.

Electrically active Nanostructures, such as carbon nanotube, silicon nanowires and nanograsses, are suitable candidates for a well-directed electrical interaction with cell outer-wall to penetrate the electric field into the cell inner parts (Xu et al., 2013)(Cohen-Karni et al., 2010). Recently, we have incorporated vertically aligned carbon nanotubes (CNT) covered microelectrodes to mechanically entrap human colon cancer cells. The entrapped cells were detected by electrical signals directly extracted from cell membrane by nanotubes (Abdolahad et al., 2012) (M. Abdolahad et al., 2012) . Also we have applied a CNT-based endoscope for metastasis diagnosis of single cancer cells based on their different electrical resonance spectroscopy (Abdolahad et al., 2013b).

In this paper, we describe the design and fabrication of a silicon nanograss covered circular blade impedance biosensor as a new lab on a chip with the ability of label free detection of rare SW48 metastatic cells in co-culture with HT29 benign Colon epithelial cancer peripheral cells (as a simulation of tumor) based on their different response to electrical current flown from nanostructures. Si nanograss arrays as strong field emitters (in comparison with bulk surface) (Malekpour et al., 2011) will improve the electrical interaction with cell membrane and inner parts. Electrical stimulation of the cells can locally depolarize the cell membrane depend on its permeability. This would alter the electrical current flow blocking, penetration and distribution

by cells membrane due to their cancerous grade based on a process known as beta dispersion. Unique morphology and structure of doped Si nanograss-based microelectrodes as well as their great compatibility with silicon fabrication technology make them a suitable electrical biosensor with the capability in sensing the slight variations in electric field. All of the measurements were compared with complete benign sample (100%HT29) as reference data. The estimated sensitivity of an array of this device with 100 wells of Si nanograssed covered sensing area (in each well) would be about 25 cancer cells in a biopsy sample of 10,000 cells.

2. Materials and methods

2.1 Sensor design and fabrication

The sensor is a silicon chip 0.5 cm in diameter that contains 100 and 250 μm wide circular shape sensing electrodes which was fabricated according a simple and cost effective process flow shown in Fig. 1. Sterile silicon wafer was used as the starting material. An oxide layer, approximately 700 nm thick, was grown on the silicon wafer using thermal oxidation in an oxidation chamber (Fig. 1-a). A 150 nm Cr layer was then deposited on the wafer using electron-beam evaporation technique as the hard mask for nano grass making (in RIE process) and doping in the electrode area. The wafer was then coated with photoresist (Shipley 1813) about 2 mm thick by spin coating to precisely define the sensing electrode as a circular window. Next, the photoresist was patterned using a single mask containing the electrode design. The wafer was left in Cr etch and then placed in HF bath for 15 and 20 s, respectively to ensure about removing Cr and oxide in electrode region (Fig. 1-b). Subsequently the patterned region has been doped in phosphorous doping furnace to form a conductive surface (figure 1-c). Some of the devices were

kept as bare electrode sensors and others were further processed nanograssed electrode fabrication. Silicon nanograss array were formed on doped electrode region by reactive ion etching (RIE) with the assistance of RF plasma and SF_6, H_2 and O_2 gases. As we reported elsewhere (Mehran et al., 2011)(figure 1-d). The grass formation is strictly dependent on the etching process, which is realized in an RF-plasma (13.56 MHz) and in the presence of oxygen, hydrogen and sulfur hexafluoride (SF_6) with successive steps of passivation and etching sub-cycles. A mixture of H_2/O_2 gases with typical flows of 100 and 85 Sccm and a Trace of SF_6 is used during the passivation step. SF_6 has been applied as the inlet gas in the etching step with typical flows of 10–40 Sccm. The plasma power and period of the passivation sub-cycle are 150 W and 50 s whereas for the etching sub-cycle such parameters are tuned at 130 W and 10 s, respectively. The combination of H_2/O_2 and SF6 during the passivation step results in the creation of a protecting layer over the sidewalls of the semi vertical silicon micro hills. Using this method, silicon nanograss arrays were obtained, with sizes down to 60 nm in width. Some electrical and structural analyses of the nanograss electrode, such as sheet resistance and XRD, were discussed in support information.

In a modified method, one can omit the Cr coating process and the SiO_2 layer would play the both role of doping and grassing (in RIE) hard mask as well as electrical passivation layer.

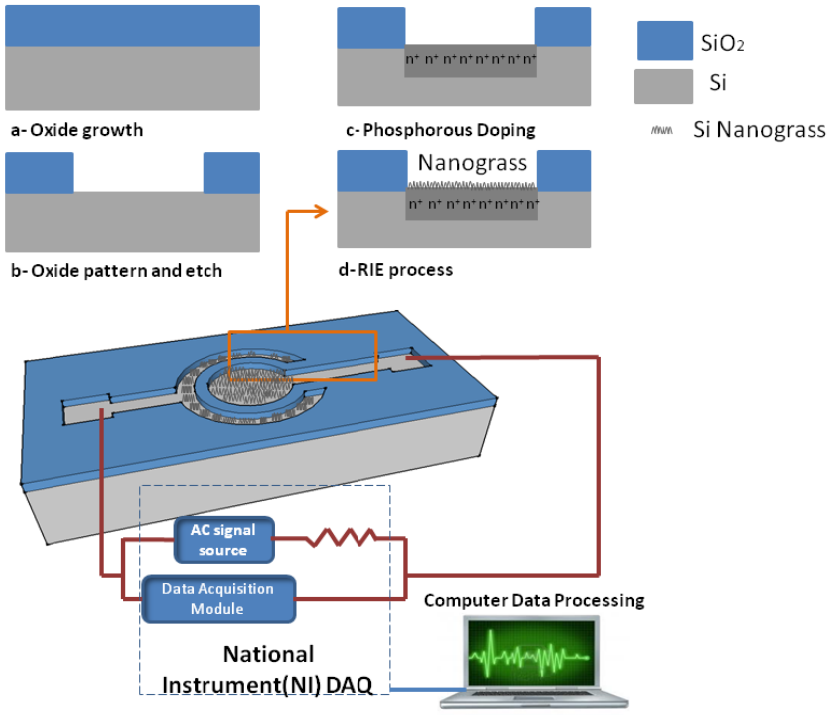

Figure1. Schematics from the fabrication process of Si nanograssed biosensor started from: (a) oxide growth on Si wafer and followed by: (b) patterning and etching the oxide in the region of the sensor. Subsequently: (c) the phosphorous dopping was achieved by doping furnace and finally: (d) Si nanograssed array was formed by RIE on the sensor region. The readout system of the sensor was schematically plotted in the bottom of the figure

Figure 2 shows an optical image of the fabricated device. A large Si nanograss covered electrode in the center was used to act as the sensing electrode which is highly receptive to the bioimpedance changes. Narrow branch of circular shape nanostructured electrode, 40 μm wide and 650 μm diameter, were designed to receive electric field emitted from cell covered sensing electrode which have been blocked or fluctuated in distribution after interaction with cells.

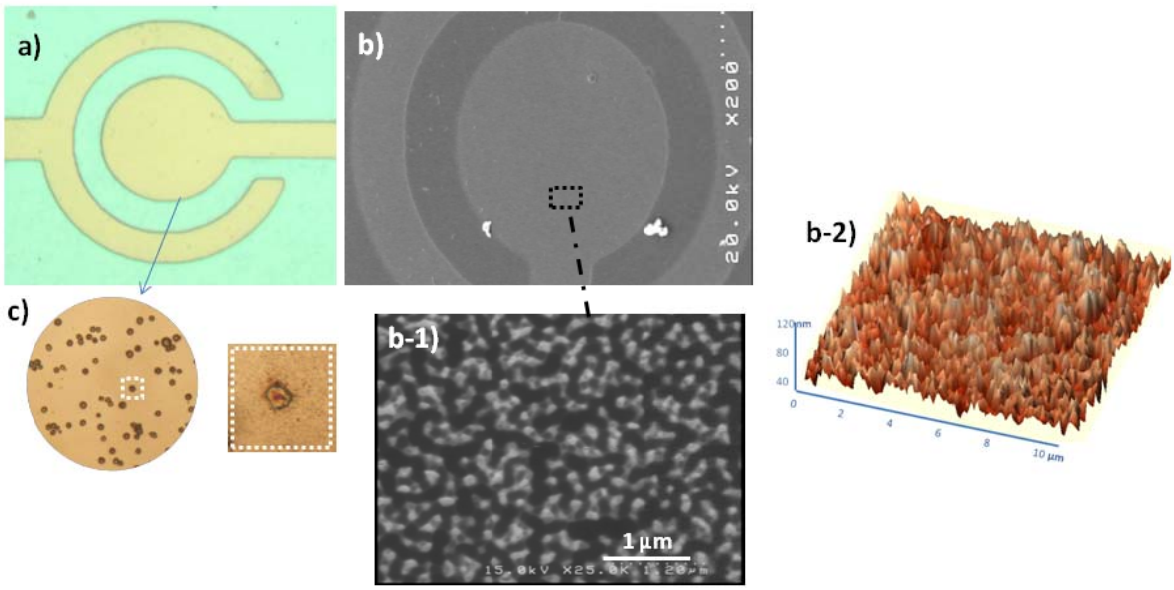

Figure2. Optical microscopy (a) and SEM images of biosensors surface. The distribution and topography of nanograssed are observable in SEM (b-1) and AFM(b-2) images respectively. (c) Optical image of electrode after cells attachment.

The wafer containing multiple devices was then diced manually to yield individual bioimpedance sensor chips. These chips were packaged with a cloning cylinder around the sensing area by affixing them with biocompatible silicon rubber to prevent the cell culture medium from leaking. The capacity of cloning cylinder is 300 µl which surrounded the sensing area and held the cell culture medium and the cells during experiments. It should be mentioned that nanostructures directly interact with cells membrane and no surface treatment was done on the electrodes to promote cell adhesion in the devices. The whole time duration of cell seeding and measurement was 4hr.

2.2 Cell culture and seeding

HT29 and SW48 cell lines as well as MCF7 and MDA-MB231 ones were obtained from the standard cell banks of national cell bank of Iran (NCBI). They were isolated from grades I and IV of human colon and breast tumors, respectively[26] and were held at 37 °C (5% CO_2, 95% air) in RPMI-1640 medium (Sigma 8758) supplemented with 5% fetal bovine serum (Gibco), and 1% penicillin/streptomycin (Gibco). The fresh medium is replaced every other day. All cells were counter stained with Hoechst 33342 dye, which stains the nucleus of the cell blue, at the end of each experiment to facilitate cell counting. Standard cell culture methods were used for cell propagation. fixed staining) In addition the HT29 (Passage 3) and SW48 (Passage 4) metastatic cells were stably transfected with green fluorescence protein (GFP) to enable us to capture fluorescent images of the electrodes and sensing area after every experiment to monitor the mixing state of different cells. In fact, the SW48 cells were tagged by GFP separately and then mixed with HT29 ones with mentioned concentrations. The resultant mixture then flowed on the sensor. In GFP protocol, FuGENE® HD Transfection Reagent (Rosche) was used to transfect the cancer cells with gWiz High-Expression GFP vector according the protocol provided by company ATCC.

The cells were counted and suspended in 100 µl of respective culture media for the monoculture experiments before being introduced into the cloning cylinder of the bioimpedance sensor. We set the cell density at 2000 cells/100 µl for the monoculture experiments. The optical microscopy images of attached cells on electrode has been shown in figure 2-c.

2.3 MTT ASSAY

The viability of the cells seeded on Si nanograssed surface were experimented by 3-(4,5-dimethylthiazol-2-yl)-2,5-diphenyltetrazolium bromide (MTT) assay conditions(Abdolahad et al., 2013a). Live/Dead viability kit (L-3224) for mammalian cells was purchased from Invitrogen (Grand Island, NY) and used to test the viability of cells under our experimental conditions. The detail of the process has been discussed in supplementary.

2.4 Bio-impedance measurement

Five individual tests were experimented in which 100% HT29 (as reference sample), 95%HT29 co cultured with 5%SW48, 90%HT29 co cultured with 10% SW48, 70% HT29 co cultured with 30% SW48 and finally 100%SW48 were seeded on the bare and nano-grassed Si electrodes with different sizes and the electrical impedance were measured to study any electrical effects of the rare metastatic cells presence on the electrode. The culture media solution of the cells contain RPMI-1640 medium (Sigma) supplemented with 5% fetal bovine serum, and 1% penicillin/streptomycin (Gibco). The bio-impedance was monitored continuously over a period of 1–4 h. During this time, the sensor was held in incubator with the parameters such as: Temperature: 37^{o}C, CO_2: 5%, relative humidity (RH): 95% (to minimize media evaporation and condensation). The primary concentration of both benign and metastatic cells was 2000#cell/ml. meanwhile the total volume of cell solution flown on the surface of each sensor was 300 µl which contain 600 #cells. The number and volume ratio of benign and metastatic cells in each experiment was indicated in the table1:

Table1. Ratio of metatstatic (SW48) Vs. benign (HT29) cells in each experiment.

Number of experiment	Percent ratio HT29 /SW48 (%)	Volume ratio HT29 /SW48 (µl)	Number of the cells HT29 /SW48 (#)	Total volume (µl)	Total number of the cells
1 (Ref. sample)	100 /0	300 /0	600 /0	300	600
2	95 /5	285 /15	570 /30	300	600
3	90 /10	270 /30	540 /60	300	600
4	70 /30	210 /90	420 /180	300	600
5	0 /100	0 /300	0 /600	300	600

Media solution has been flown on the surface of the sensor after 4 hr, to remove any nonattached cells from the surface and being ensured from cell attachment on the nanograss array. Finally just well seeded cells on the nanograss surface would be remained.

Measurements were collected over a frequency range of 100 Hz to 200 kHz by an NI USB 6353 system every one hour from each of the different cells covered devices in the culture chamber. After the final bio-impedance measurement, fluorescent images of the entire sensing area were captured (Carl-Zeiss AxioLab A1Microscope). Total numbers of benign and metastatic cells on the electrode were counted using these images and compared with electrical measurements. For each electrode, the normalized impedance values and the number of metastatic cells on the electrode responsible for the bio-impedance fluctuation from reference value (completely benign cells with same concentration) were tallied. To investigate the repeatability of the electrode, we repeated the biological tests on the device and investigated the surface after each cell detachment sequence by AFM and EDX analyses. More details have been discussed in support information.

3. Results and discussion

3.1 physical and biological characterization of the Si nanograss

Figure 2-b represented the SEM image of the Si nanograss surface. The feature size of the grasses is less than 100 nm with a homogeny distribution all over the surface (fig 2-b-1). Also as shown in AFM topography (fig 2-b-2), the mean height of the grass nano hills are about 80 nm.

In addition the Biocompatibility results of Si nanograsses investigated by MTT assays show more than 94% viability of the seeded cells after 24hrs in comparison with control sample as discussed in supplementary (Fig S1).

3.2 Detecting the presence of rare metastatic cells

Figure 3-a shows the diagram of impedance difference (ΔZ) between the primary cancerous HT29 cells sample with the concentration of 100% (as reference sample) and the HT29 cells co-cultured with 10% and 30% of metastatic SW48 cells with the same total concentration (2000 cell#/ml) seeded on Si nanograss sensing electrodes, respectively. The scanning frequencies were ranged from 0.1 to 200 kHz. Also the impedance difference between reference sample and the sample contains 100% SW48 cells was experimented as estimation for the electrical response of a completely metastatic sample. The diameter of the electrode was 250 μm and the time duration of the seeding processes were 4 hr. As it has been elaborated in figure 3-b, when the presence of SW48 metastatic cells in the benign HT29 sample was 10%, ΔZ varied from 1100 to 200 Ω over the frequencies ranged from 20 to 200 kHz respectively. After increasing the metastatic cells to 30%, the values of ΔZ was raised to 1460 Ω at 20 kHz and reached to 300 Ω at 200 kHz. In fact, the most changes in ΔZ after changing the presence of SW48 cells from 10% to 30%, has been

occurred in the frequency of 50kHz as the exact diagnosis frequency (Figure 3-b-1). This frequency clearly represents the relationship between the metastatic cells concentration and ΔZ. When the percent of metastatic SW48 cells was enlarged to 100%, the ΔZ observably enhanced and ranged from 45 to 5 kΩ in the mentioned series of frequencies. The GFP tagged rare metastatic cells with the concentrations of 10% and 30% among primary cancerous ones on the surface of the electrodes are observable in the microscopy images of figures 3-c and 3-d respectively.

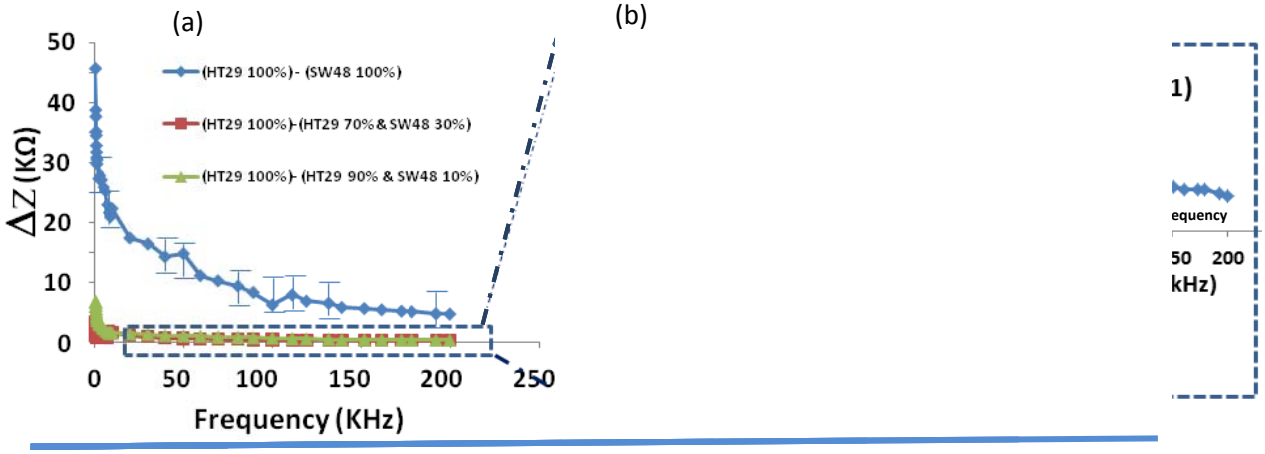

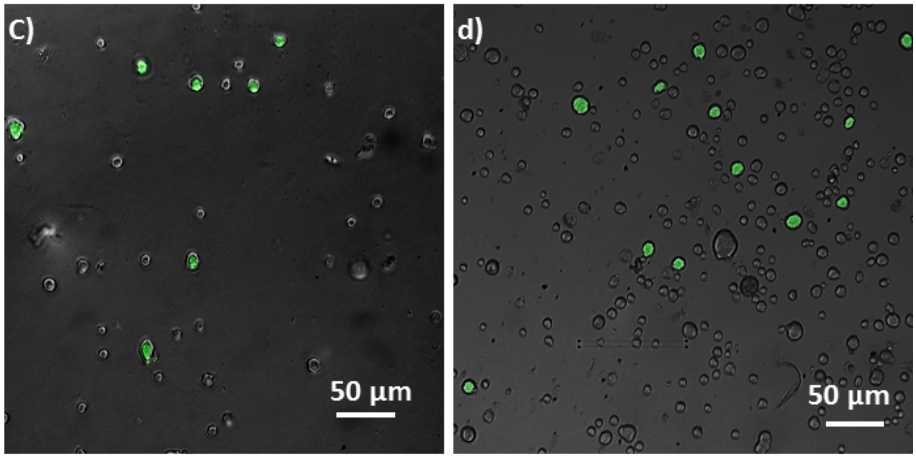

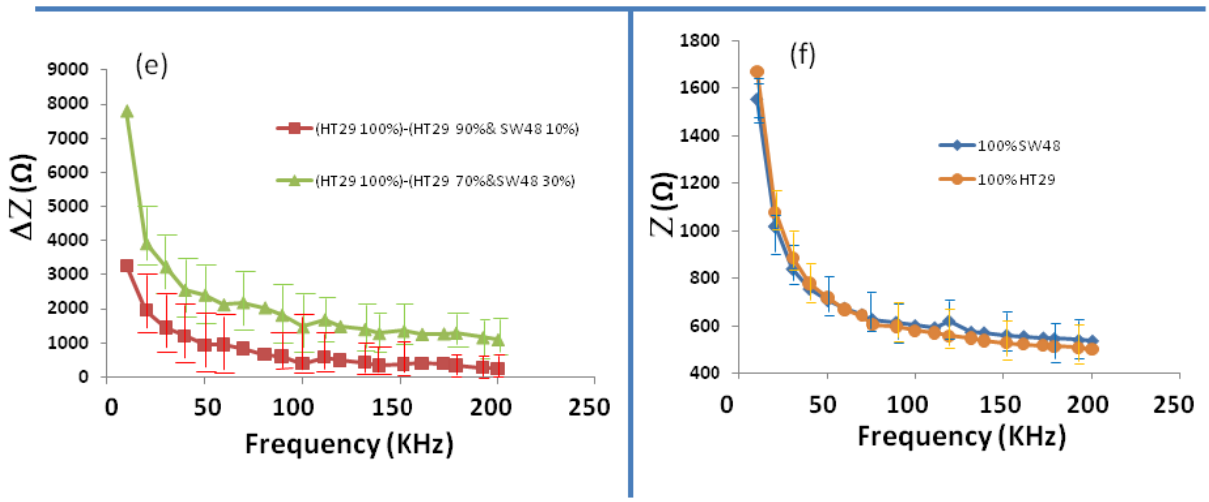

Figure 3. (a)The impedance difference (ΔZ) results between primary cancerous colon cells (HT29) as reference sample and it's mixed culture with rare metastatic ones (SW48) with 10% and 30% concentrations measured by Si nanograss based electrical biosensor (with the diameter of 250 µm) at different probe frequencies. Also the ΔZ between reference and 100% SW48 samples was measured. The total cells concentrations of all samples were 2000cell#/ml. The ΔZ has been enhanced by increasing the concentration of metastatic cells. (b) ΔZ of the samples with 10% and 30% SW48 metastatic cells from reference data in higher resolution. An increment in the concentration of metastatic cells from 10% 30% resulted in about 400Ω increment in ΔZ. Mean standard deviation bars:+/- 90Ω. (b-1) Diagram of ΔZ differences between the samples contain 10% and 30% metastatic cells in the same range of frequencies. The best alterations in ΔZ have been occurred in 50kHz as the exact diagnosis frequency. in impedance difference Fluorescence microscopy image showing the spreading of 10% (c) and 30% (d) SW48 cells on the electrode in co-culture experiments. The metastatic SW48 cells are GFP tagged before mixing whereas shown with a green trace mean while the HT29 cells weren't tagged by any markers and were seen uncolored. (e) Bioimpedance detection of rare metastatic cells (10% and 30%) in co-culture with primary ones on the silicon nanograss covered microelectrode with the diameter of 100µm. standard mean dev.: =/- 110 Ω (f) Impedance diagram of 100% SW48 and 100% HT29 separated cells samples with same total concentrations experimented by bare Si microelectrode, no observable impedance changes was detected by bare Silicon surface. Standard mean dev.: =/- 105 Ω.

3.3 Electrode size effect in the response

As shown in figure 3-e, the ΔZ were increased observably when the diameter of the nano-grassed covered electrode reduced from 250μm to 100μm (in comparison with figure 3-b). In such size of electrodes (100μm), when the concentration of metastatic cells are 10%, the ΔZ was varied from 3500 to 200 Ω in the frequencies ranged from 10 to 200 kHz. By increasing the percent of metastatic cells to 30%, the ΔZ has been varied from 8000 to 300 Ω in the same range of frequencies. The smaller electrode allows larger current densities to flow (Arya et al., 2012). When such electrode experiences surface current blockage due to the presence of a cell, the reduction in surface current is dramatic. More investigations about the effect of electrode size on the response of the device were discussed in supplementary. In the case of bare doped silicon electrode (silicon surface with no nanograss covered on), no observable change in the impedance was determined even between the 100% SW48 cells sample and reference (100% HT29) one which was ranged from 100 to 30 Ω at same frequencies (figure 3-f).

3.4 Beta dispersion differences, the mechanism of metastatic cells sensing

Beta dispersion as one of intrinsic bioelectrical properties of the cell membrane in response to AC electrical excitation is one of the key parameters involve in our diagnosis approach. This phenomenon is related to the ability of a biological cell membrane in filtering out low frequency currents and allowing high frequency ones to pass through (Francis, 2006.). We know that cell membrane naturally has capacitance which makes it a frequency-dependent conductor.

Beta dispersion of a cell, associated with the polarization of cellular membranes, is depending on the dielectric properties of the cell membrane and inner parts. Due to the dielectric parameters

disruption of the cell during cancerous transformation (Abdolahad et al., 2013b), beta dispersion have a strong correlation with the grade of the cancer cell. The amount of current flow blocking by the electrical excited cells is different due to their membrane and cytoplasm dielectric properties depend on cancer progression. Metastatic cells have less ability in blocking the current flow into their membrane and their beta dispersion effects are different from healthy cells. On the other hand, when a cell grows on the conventional electrode (such as Au or ITO microelectrodes), adhesive contacts are formed, which account for 15-20% of the cell surface area(Huang et al., 2004). Creation of nano-rough features increases surface energy leading to greater secreted protein (such as vitronectin and fibronectin) interactions to improve specific cell attachment sites (Ko et al., 2013). So, the cell-surface nano contacts area would improve the electrical interactions between the cell membrane and tips of nanograss array. In this manner, the highly conductive tips of nanograss could extract impedance signals through cell membrane. So, we can accurately sense any slight variations in current flow caused by cell membrane through beta dispersion (figure 4-a), to diagnose the presence of metastatic cells in whole benign sample (figures 4-b and c). It is worth noting that the strong adhesion of cells to nano-textured surfaces is not observed for bare silicon micro electrode. As a result, we were not able to detect minor fluctuations in current especially at higher frequencies (more schematics have been elaborated in figure S2 of supplementary).

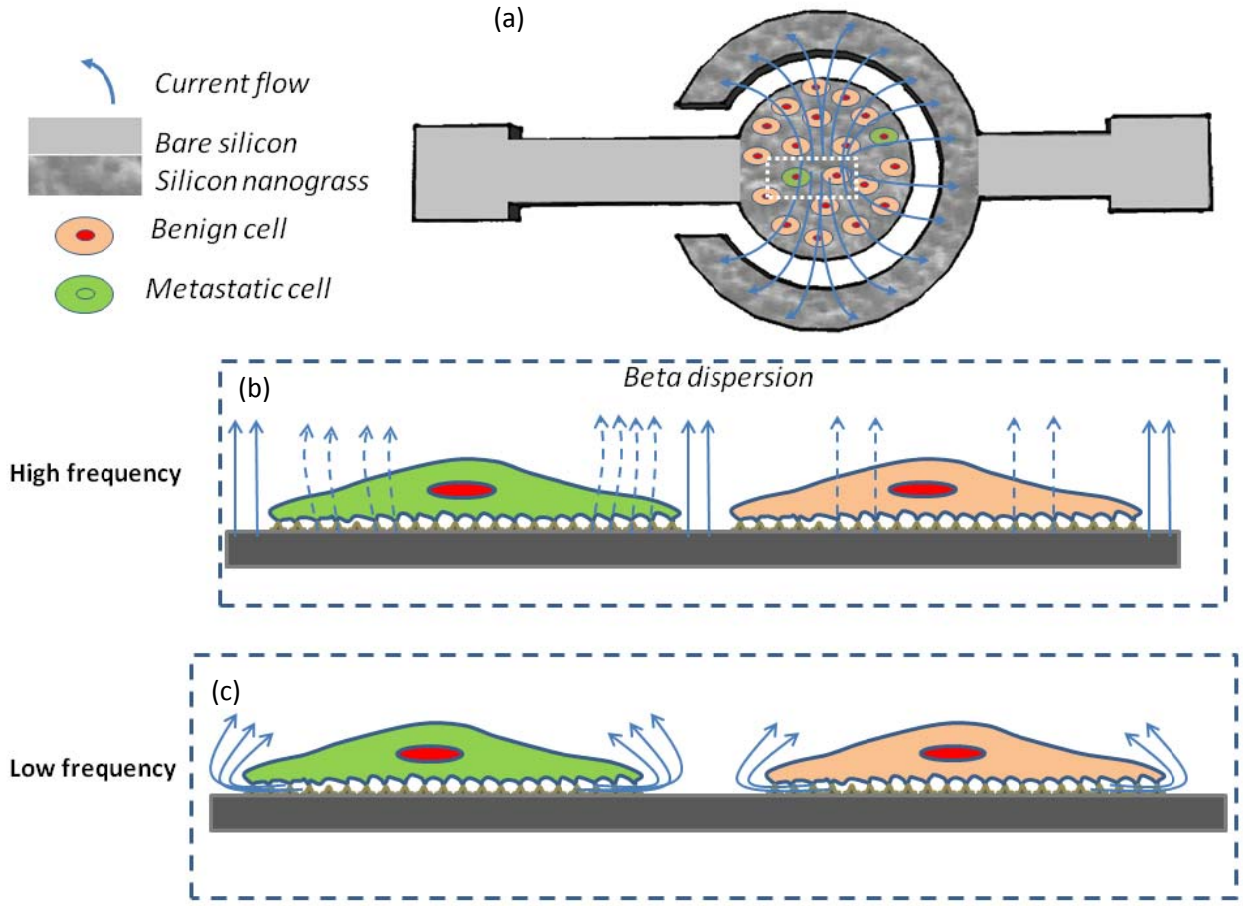

Figure 4. (a) Schematic of current flow in Si nanograss based biosensor. In high frequency regime the current flow blocking through beta dispersion mechanism is weaker in metastatic cells and higher fraction of currents will penetrate to them in comparison with primary cancerous ones (b). In low frequency regimes most of the currents flow through the culture media (c) due to interface faradic impedance.

3.5 Impedance phase diagram

Other than impedance value diagram, impedance phase would be another indication for cancer detection proposes(Gupta et al., 2004). The phase value directly related to the dielectric parameters of the investigated cells. It can reflect more accurate data about the membrane disruption of the cell during metastasis progression (Abdolahad et al., 2013b). As shown in figure 5-a, Even 5% rise in the presence of rare metastatic cells was detected in impedance phase

diagram of the Si nano-grassed based biosensor with the electrode diameter of 100 µm. 5% increment in the concentration of metastatic cells reduced the impedance phase (φ) in the range of 4 to 10 ^{o} in comparison with reference sample in the frequencies ranged from 50 to 200 kHz. Further increment in the concentration of metastatic cells to 30% of the total cells abridged the φ in the range of 14 to 20^{o} in the same series of frequencies. In the case of bare Si electrode, no noticeable Δφ has been observed even between 100% metastatic SW48 and reference (whole HT29) samples which was less than 10^{o} in the frequencies lower than 10 kHz and less than 4^{o} in the frequencies ranged from 50 to 200 kHz respectively (fig 5-b.). Such measurements corroborate the ability of nano-grassed doped Si electrodes in label free tracking the rare metastatic cells in benign sample which were not achieved before. The fluorescent microscopy image shown in figure 5-c, presented the HT29 uncolored cells co cultured with 5% of GFP tagged SW48 metastatic cells seeded on the surface.

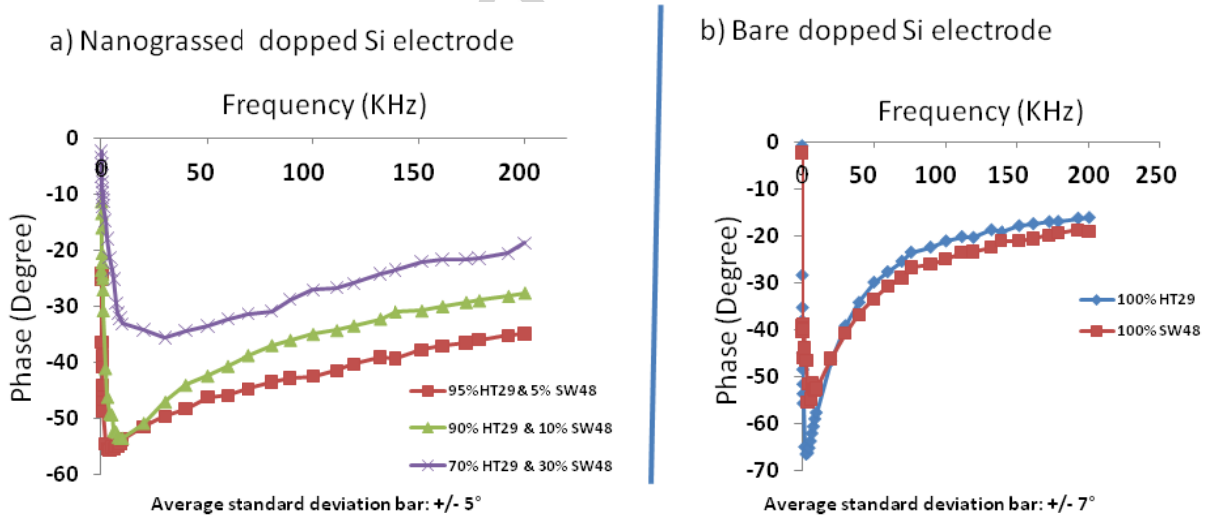

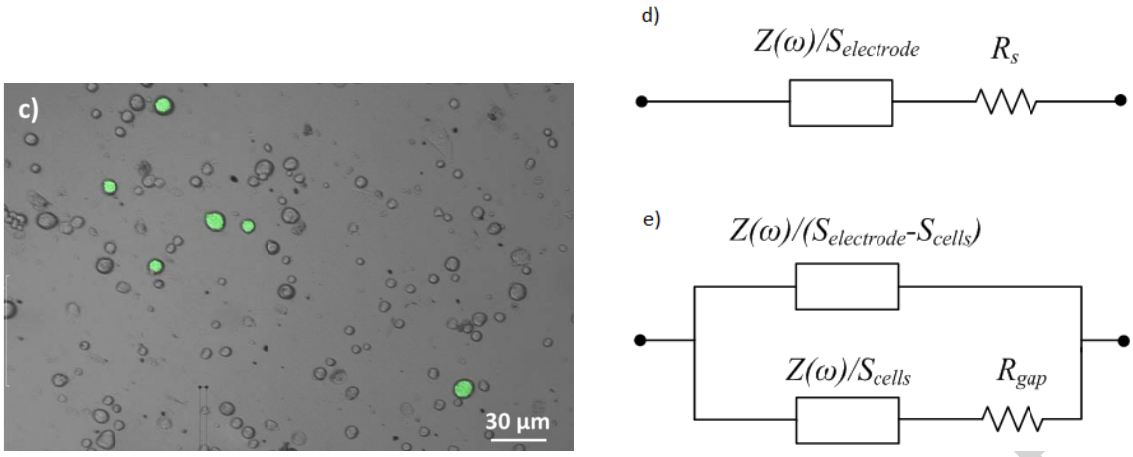

Figure 5. (a) impedance phase diagram from Si nanograss based biosensor covered by commixing of HT29 - SW48 cells with the concentrations of 95%-5% , 90%-10% and 70%-30% respectively. The delta phi has been obviously reduced even by 5% increment in the presence fraction of SW48 cells. (b) No observable change in the impedance phase value has been measured between 100%HT29 and 100% SW48 cells samples covered on bare Si microelectrodes. (c) Fluorescence microscopy image from GFP tagged SW48 cells with the concentration as rare as 5% co cultured with non-tagged HT29 cells. Equivalent circuit model of cell covered microelectrodes in (c) low and (d) high frequency regimes.

3.6 Equivalent Circuit model of the device

Media culture liquid forms an electrified double layer at the interface of circular electrode due to the chemical reactions (Bockris, 2000). Two parameters will affect the current signal to pass through the electrified interface. First, faradic impedance as the result of electron exchange at the interface and second, capacitive current flow through the double layer. The impedance of electrode interface has an inverse relation to the electrode area and is frequency dependent (*Cell-based Biosensors: Principles and Applications*, 2009), which can be represented by $Z(\omega)/S_{electrode}$. The total impedance of the sensor depends on the interface faradic impedance and the media culture resistance named as spreading resistance (R_S) in their series connection, as shown in figure 5-d. R_s is inversely related to the square root of electrode area and is frequency independent. At low frequencies, faradic interface impedance is the main effective element (Huang et al., 2003).

As frequency increases, the spreading resistance will be dominated over the faradic impedance. The cell membrane is a highly dielectric layer. So, after cells attachment on the

electrode, the current flowing from the cell-covered region (S_{cell}) couldn't penetrate the membrane and flows through the resistive gap area existed between the surface and cells outer membrane modeled by a resistance (R_{gap}). The attachment of cells will divide the electric field diffusion into two branches, the cell diffused electric field fraction with impedance of $Z(\omega)/S_{cell}$ in series with R_{gap}, and culture media liquid diffused fraction with impedance of $Z(\omega)/(S_{electrode}-S_{cell})$ (figure 5-e).

In the case of nanograss electrode, the well focal adhesion and stretching of cells on the surface as well as direct noncontacts which have been just applied between tips of nanograsses and cell membrane, would reduce the cell-surface gap region (figure 6-a and SEM images of figure 6-b and b-1) and restrict the current flow through media solution. Hence, It would result in lower R_{gap} and improve the role of Z_{cell} in final impedance in comparison with bare electrodes. The SEM and AFM images presented in figure 6-b and c respectively, elaborate the well focal adhesion of nano contacts applied between the membrane of seeded cell and nanograssed Si in comparison with bare Si surface (schematic of figure 6-d and AFM of figure 6-e).

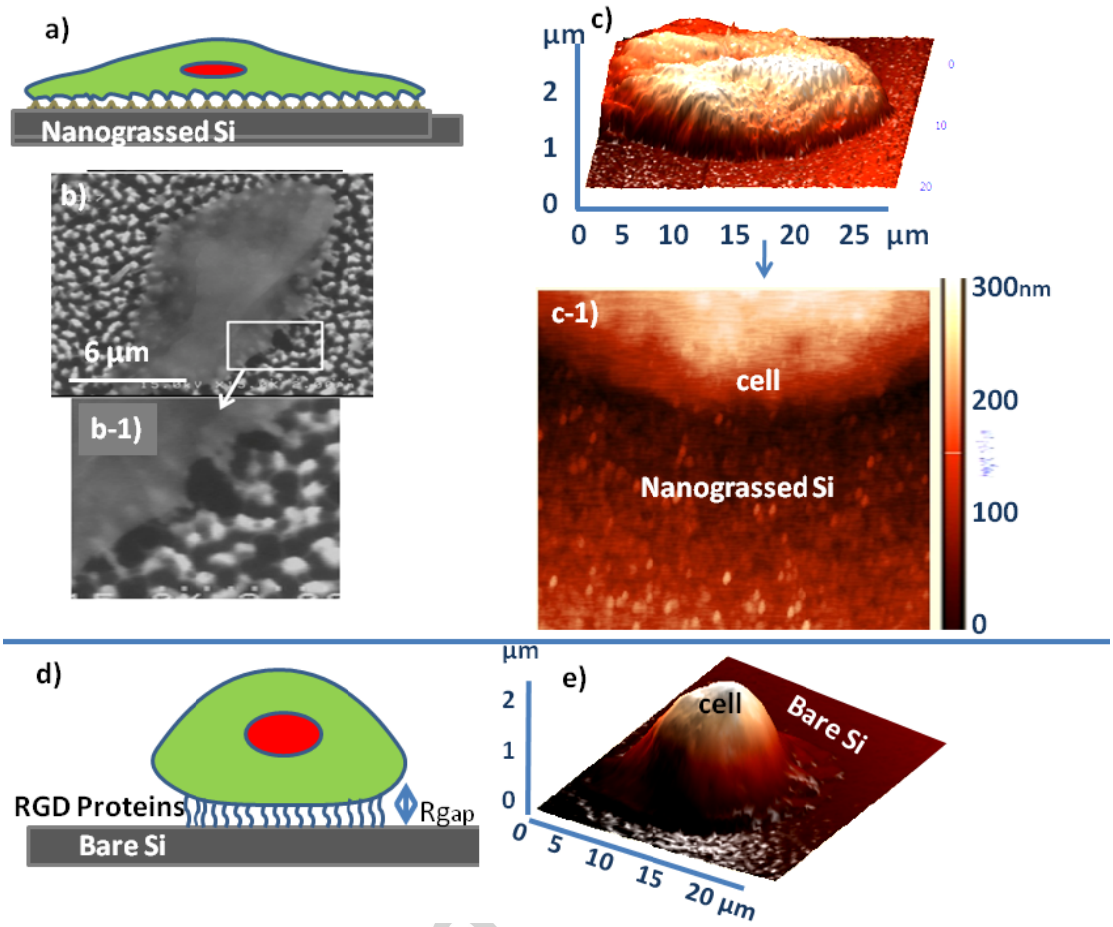

Figure 6. (a) schematic of nano contact adhesion sites applied between cell membrane and tips of Si nanograss surface. (b) SEM image of cancer cell attached on Si nanograss surface in which these nanocontacts are observable (b-1). (c) AFM topography from cancer cell seeded on nanograss surface spreading of the cell and nanocontact between cell and tips of nanograss (c-1) are noticeable. (d) Schematic of the cell attached on bare Si surface. € AFM topography of cancer cell attached on bare Si surface in which cell spreading and focal adhesion wasn't occurred such as nanograss surface.

On the other hand, as we previously reported (Abdolahad et al., 2013b) because of the membrane disruptions occurred in metastatic cells, they couldn't effectively block the current flow through themselves when electrically have been excited, so the impedance of the electrode after the presence of metastatic cells will be reduced and impedance difference from the reference sample

(ΔZ) will be increased as the metastasis indication. Nanograss architecture of the Si electrode greatly reflects any fluctuation in z_{cell} due to the presence of metastatic cells.

The time evolution of impedance measurements show a well stability for the device as discussed in support information (figure S3-a). The ΔZ between reference sample and its mixture with rare concentrations of metastatic cells has been held even after 24hr (figure S3-b).

To more clearly disclose the impedance change of the electrode due to the presence of rare metastatic cells, the normalized impedance change diagram was plotted and discussed in detail in supplementary (figure S4) which shows a well demand with beta dispersion mechanism.

4. Conclusion

This work presents an electrical nano biosensor fabricated by doped silicon nanograss array with the ability of label free detecting the rare human metastatic colon cells in a background of benign ones. The detection mechanism based on different current flow blocking by metastatic cell membrane in comparison with benign one due to beta dispersion phenomenon which results in impedance changing of the sensor. Nano contact adhesive sites have been applied between cell membrane and tip of silicon nanograss, investigated by AFM and SEM images, play the key role in this system. The sensor is capable to detect as low as 5% metastatic colon cells among total sample. Bioimpedance sensing using this type of diagnostic device has potential application in the analysis of wide variety of samples such as fine needle aspirates, cancer involved cells biopsy and fluid samples (bile secretion for cholangiocarcinoma or urine for bladder cancer) for more accurate cancer staging instead of expensive marker based pathological methods.

References

Abdolahad, M., Janmaleki, M., Mohajerzadeh, S., Akhavan, O., Abbasi, S., 2013a. Mater. Sci. Eng. C. Mater. Biol. Appl. 33, 1498–505.

Abdolahad, M., Janmaleki, M., Taghinejad, M., Taghnejad, H., Salehi, F., Mohajerzadeh, S., 2013b. Nanoscale 5, 3421–7.

Abdolahad, M., Sanaee, Z., Janmaleki, M., Mohajerzadeh, S., Abdollahi, M., Mehran, M., 2012. Carbon N. Y. 50, 2010–2017.

Abdolahad, Mohammad, Taghinejad, M., Taghinejad, H., Janmaleki, M., Mohajerzadeh, S., 2012. Lab Chip 12, 1183–90.

Alexe, G., Alexe, S., Axelrod, D.E., Bonates, T.O., Lozina II, Reiss, M., Hammer, P.L., 2006. Breast Cancer Res 8, R41.

Arya, S.K., Lee, K.C., Bin Dah'alan, D., Daniel, Rahman, A.R.A., 2012. Lab Chip 12, 2362–8.

Asami, K., 2002. Prog. Polym. Sci. 27:1617-1659 7

Bockris, J.O., 2000. Modern Electrochemistry 2B: Electrodics in Chemistry, Engineering, Biology and Environmental Science, Volume 2. Springer.

Cell-based Biosensors: Principles and Applications, 2009. . Artech House.

Chen, J., Zheng, Y., Tan, Q., Shojaei-Baghini, E., Zhang, Y.L., Li, J., Prasad, P., You, L., Wu, X.Y., Sun, Y., 2011. Lab Chip 11, 3174–3181.

Cheung, K., Gawad, S., Renaud, P., 2005. Cytometry. A 65, 124–32.

Cohen-Karni, T., Qing, Q., Li, Q., Fang, Y., Lieber, C.M., 2010. Nano Lett. 10, 1098–102.

Cristofanilli, M., De Gasperis, G., Zhang, L., Hung, M.-C., Gascoyne, P.R.C., Hortobagyi, G.N., 2002. Clin. Cancer Res. 8, 615–619.

Du, E., Ha, S., Diez-Silva, M., Dao, M., Suresh, S., Chandrakasan, A.P., 2013. Lab Chip 13, 3903–3909.

Fischer, A.H., Jacobson, K.A., Rose, J., Zeller, R., 2008. CSH Protoc. 2008, pdb.prot4986.

Francis, T., 2006. Handbook of Biological Effects of Electromagnetic Fields, Third Edition - 2 Volume Set (Hardback) - Taylor & Francis.

Frazier, A.B., Chen, Z.G., Han, A., 2009. J. Microelectromechanical Syst. 18, 808–817.

Gupta, D., Lammersfeld, C.A., Burrows, J.L., Dahlk, S.L., Vashi, P.G., Grutsch, J.F., Hoffman, S., Lis, C.G., 2004. Am. J. Clin. Nutr. 80, 1634–1638.

Han, C., Lampert, A., Rush, A.M., Dib-Hajj, S.D., Wang, X., Yang, Y., Waxman, S.G., 2007. Mol. Pain 3, 3.

Heileman, K., Daoud, J., Tabrizian, M., 2013. Biosens. Bioelectron. 49C, 348–359.

Hu, Y., Zuo, P., Ye, B.-C., 2013. Biosens. Bioelectron. 43, 79–83.

Huang, X., Greve, D.W., Nguyen, D.D., Domach, M.M., 2003. Proc. IEEE Sensors 2003 (IEEE Cat. No.03CH37498) 1.

Huang, X.H.X., Nguyen, D.N.D., Greve, D.W., Domach, M.M., 2004. IEEE Sens. J. 4.

Ko, T.-J., Kim, E., Nagashima, S., Oh, K.H., Lee, K.-R., Kim, S., Moon, M.-W., 2013. Soft Matter 9, 8705.

Kunzelmann, K., 2005. J. Membr. Biol. 205, 159–73.

Lan, K.-C., Jang, L.-S., 2011. Bioelectron. 26, 2025–31.

Ling, J., Wiederkehr, U., Cabiness, S., Shroyer, K.R., Robinson, J.P., 2008. Diagn Cytopathol 36, 76–84.

Malekpour, H., Mehran, M., Mohajerzadeh, S., 2011. The Electrochemical Society, pp. 347–351.

Mehran, M., Sanaee, Z., Abdolahad, M., Mohajerzadeh, S., 2011. Mater. Sci. Semicond. Process. 14, 199–206.

Murray, N.P., Calaf, G.M., Badínez, L., 2009. Oncol. Rep. 21, 571–575.

Pick, H., Terrettaz, S., Baud, O., Laribi, O., Brisken, C., Vogel, H., 2013. Biosens. Bioelectron. 50, 431–6.

Pokorný, J., 2012. AIP Adv. 2, 011207.

Saliba, A.-E., Saias, L., Psychari, E., Minc, N., Simon, D., Bidard, F.-C., Mathiot, C., Pierga, J.-Y., Fraisier, V., Salamero, J., Saada, V., Farace, F., Vielh, P., Malaquin, L., Viovy, J.-L., 2010. Proc. Natl. Acad. Sci. U. S. A. 107, 14524–9.

Scaglia, N., Caviglia, J.M., Igal, R.A., 2005. Biochim Biophys Acta 1687, 141–151.

Sivagnanam, V., Song, B., Vandevyver, C.D.B., Bünzli, J.-C.G., Gijs, M.A.M., 2010. Langmuir 26, 6091–6096.

Srinivasaraghavan, V., Strobl, J., Agah, M., 2012. Lab Chip 12, 5168–79.

Valero, A., Braschler, T., Renaud, P., 2010. Lab Chip 10, 2216–2225.

Vu, X.T., Susloparova, A., Weil, M., Koppenhöfer, D., Ingebrandt, S., 2012. Biosens. Bioelectron.

Xu, L., Jiang, Z., Qing, Q., Mai, L., Zhang, Q., Lieber, C.M., 2013. Nano Lett. 13, 746–51.

Yang, L., Arias, L.R., Lane, T.S., Yancey, M.D., Mamouni, J., 2011. Anal. Bioanal. Chem. 399, 1823–33.

Research Highlights

►This paper evaluates a silicon based nanobiosensor for detection of rare invasive cancer cells.

►Nano contacts applied between doped silicon nanograss and cell membrane have the key role in detection.

►Beta dispersion, an intrinsic electrical property of the cell membrane, is the specific parameter in diagnosis approach.